Introduction

Hydrocarbon gas extracted from the Snohvit gas field contains approximately 6% CO_2. The gas is piped to shore 150 km away for processing before the extracted CO_2 is returned by pipeline for injection. In this study, analysis of the Snohvit CO_2 injection program relates to the period prior to the 2009 3D seismic monitoring survey. This followed the injection of 0.5 Mtons of CO_2 over 16 months at the base of the Tubaen Formation, a fluvial to tidal sandstone deposit of approximately 100 m thickness. This formation, at a depth of 2565-2665 m below sea surface lies beneath the producing Snohvit gas field. The reservoir proved to be more complex than originally anticipated with significant permeability variations. These have been attributed to quartz cementation, fluvial channelling and the possibility of undetected faults in the formation hindering flow. Horizontal permeabilities range from mDarcies to several Darcies whilst porosity values between 8 % and 20 % are observed (Hansen et al., 2011). Log records confirm that the unit also contains four thin mudstone layers which appear to have hindered flow into the less permeable upper Tubaen.

The 3D seismic surveys utilised in this study were collected in 2003 and 2009 and are both orientated North-South. A shared lateral extent of 8.25 km x 9.65 km is analysed. Source steering ensured an excellent match of source and receiver locations between the 2003 and 2009 data and repeatability metrics are high. Seismic cross-sections from the data are displayed in Figure 1 and intersect the injection point. The top Tubaen reflection is poorly imaged on the seismic data with the overlying top Fugeln acting as a regional indicator. The base Tubaen is imaged across the survey area. Facies and porosity changes in the Tubaen are thought to account for variable amplitudes in the baseline survey.

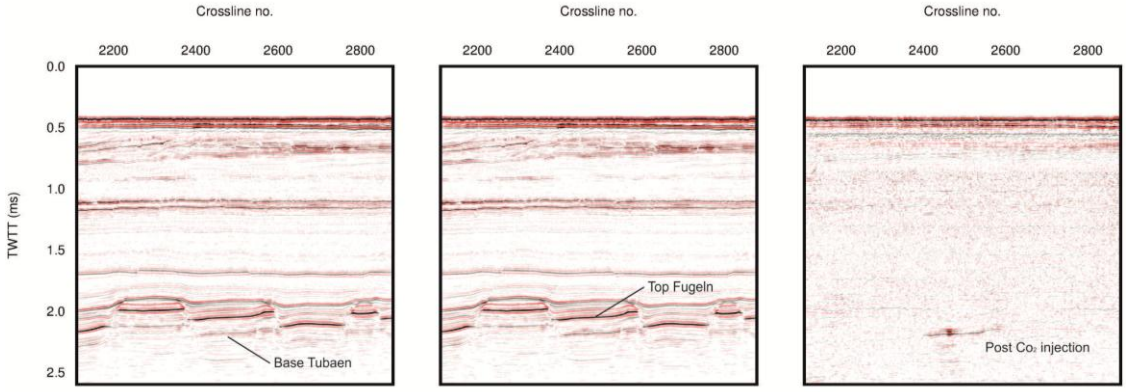

Figure 1. *Seismic sections from the 2003 baseline (left), 2009 repeat (middle) and difference (right) data cubes*

Figure 2 shows amplitude plots of the base Tubaen from the 2003 and 2009 surveys in plan-view alongside a plot of the difference between the two grids. The effect of CO_2 injection is clearly evident, with the greatest amplitude differences evident close to the injection perforations and on the margins of previous amplitude highs. This suggests subsurface changes preferentially occur in regions of greater permeability and porosity. Due to the lateral extent of the difference anomaly it has been postulated that a pressuring-up of the pore water is responsible for the majority of the difference signal (Hansen et al., 2011). If fluid substitution, that is CO_2 replacing brine, were responsible for the entire extent of the anomaly, the CO_2 layer could be at most 1-2 meters thick and beneath the limit of detection with the frequency and noise content of the seismic data. However, if a smaller CO_2 saturated zone is located close to the injection point, pooled in the lower Tubaen beneath the deepest intra-Tubaen thin mudstone layer, the spectral content of the data should provide some clues as to its extent.

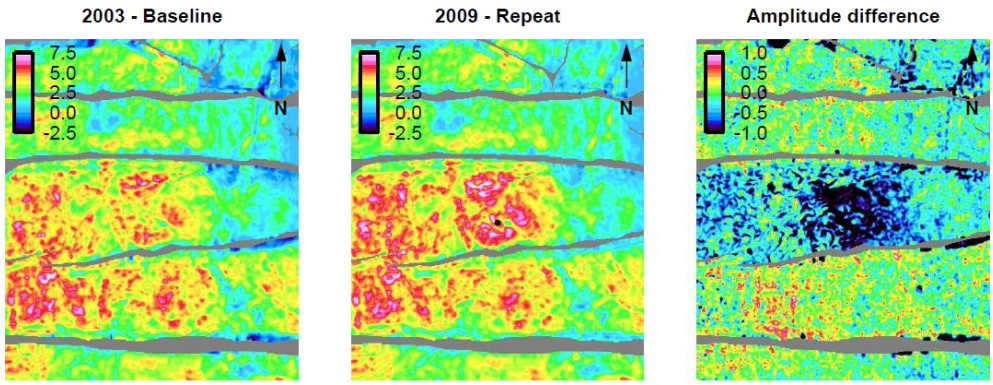

Figure 2. *Reflection amplitudes for the base Tubaen extracted from the baseline (left) and repeat (middle) monitoring surveys at Snohvit. The difference between the grids is displayed on the right. The injection point is shown with a black dot in the middle image.*

Method

Anomalies of differing temporal thickness will tune different frequencies in the seismic wavelet – boosting their amplitude. Determining which frequencies have been tuned allows the thickness of the causative layer to be inferred. The pressure is likely to have a greater vertical extent than the saturation change (which will be restricted to thin layers of CO_2) and will therefore cause preferential tuning at lower frequencies. This study postulates that by assessing the spatial variation in peak tuning frequency around the base Tubaen reflection it should be possible to separate the saturation and pressure effects; whilst acknowledging that the pressure response will be laterally coincident with that from the fluid changes and may generate some signal masking.

In order to isolate the spectral content of reflection pairs arising from individual layers of CO_2 it is necessary to extract data from a short time window. Williams and Chadwick (2012) undertook an assessment of various spectral windowing techniques and established that a suitable trade-off between temporal windowing and spectral resolution was achieved with the quadratic smoothed pseudo Wigner-Ville distribution (SPWVD).

$$SPWVD_{x(t,v)} = \int_{-\infty}^{+\infty} h(\tau) \int_{-\infty}^{+\infty} g(x-t)x\left(t+\frac{\tau}{2}\right)x^*\left(t-\frac{\tau}{2}\right)dt\, e^{-i2\pi f\tau}d\tau$$

where t is time, τ the lag, *f* the frequency and g(x-t) and h(τ) are smoothing kernels along the time and frequency axes respectively and * represents complex conjugation. White et al. (2013) previously utilised the scheme during investigations into CO_2 layer thickness estimation at Sleipner.

Analysis

Single-frequency reflection amplitude data cubes were generated from both 3D time-lapse seismic data sets. The base Tubaen reflection was used to extract amplitudes from the correct horizon. Noting the band-limited nature of the seismic wavelet, spectral balancing was undertaken. Under the assumption that geologic tuning of every discrete frequency occurs somewhere within the seismic volume, the wavelet spectrum can be balanced by equalizing each frequency slice according to its maximum amplitude in the overlying seismic section (Partyka et al., 1999). This technique is termed 'frequency normalisation' and slices from the normalised time-lapse data sets are shown in the upper and middle rows of Figure 3.

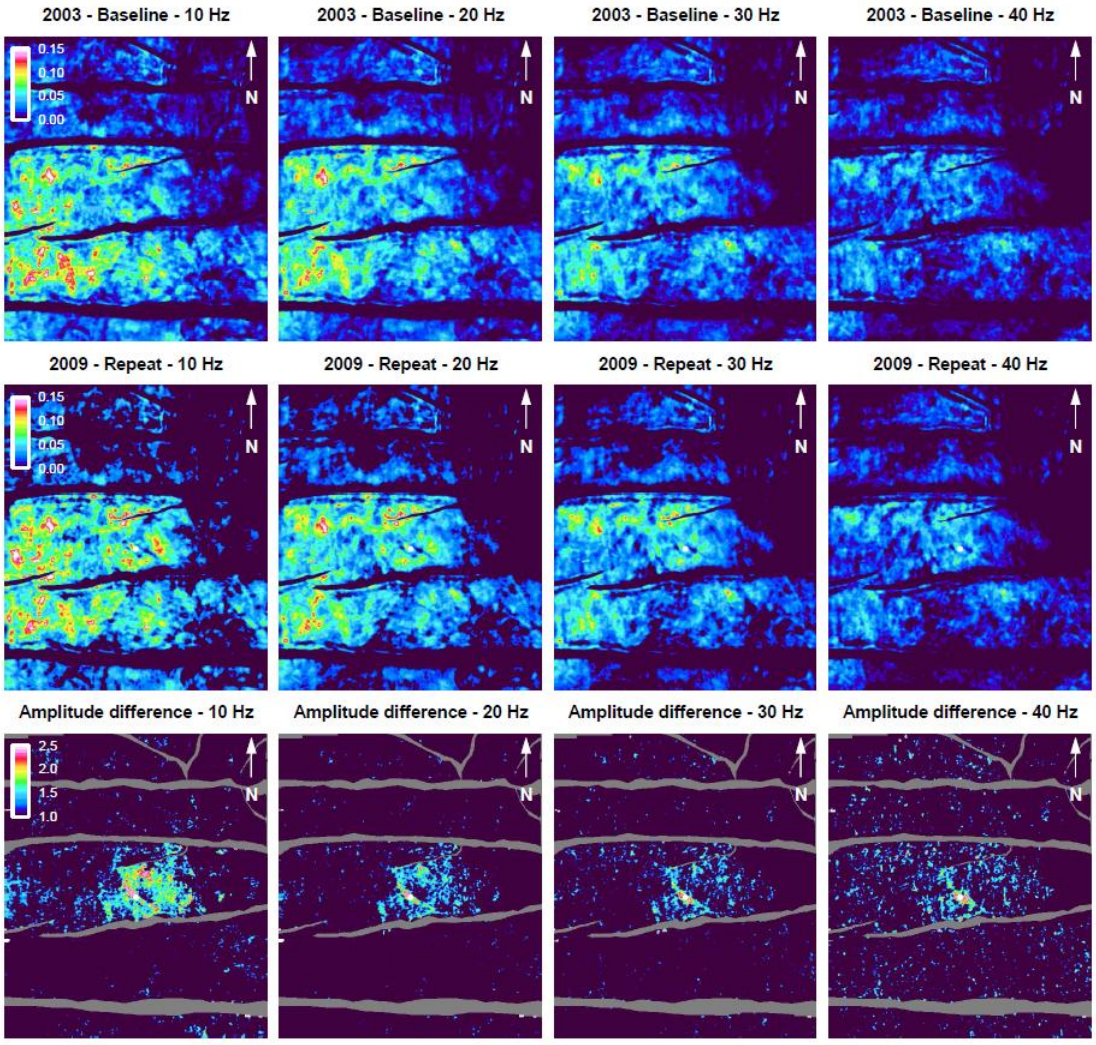

Figure 3. *Frequency normalized reflection amplitudes for discrete frequency slices from pre-injection survey (top) and repeat survey (middle) and the amplitude normalised difference plots for discrete frequency slices from repeat survey (bottom).*

In order to assess the change in frequency content of the time-lapse signal an 'amplitude normalisation' is undertaken, normalising the repeat survey by the baseline response. The results are displayed on the bottom row of Figure 3 and show that a reduction in the lateral extent of the difference anomaly is evident as frequency increases. This supports the hypothesis that the pressure increase occupies a greater vertical extent, and has a significantly larger spatial footprint than the fluid substitution change since a thicker pressure anomaly would tune at lower frequencies.

In order to separate the pressure and saturation effects a spatial analysis of 'frequency displaying the largest change in amplitude' is undertaken. Figure 4 (a) shows how this metric varies over the survey area. Fluid substitution changes are expected to occur in thin layers, so reponses seen at over 25 Hz are likely to be derived primarily from the emplacement of CO_2. The pressure signature is expected to extend into the middle and upper regions of the reservoir so it is proposed that where the greatest change is below 25 Hz a pressure increase is responsible. Figure 4 (b) and (c) highlight this separation and justify the hypotheses that the CO_2 will remain close to the injection site.

The separation of pressure and saturation contributions to the seismic response at Snohvit has been considered previously. Hansen et al. (2011) used simple AVO analysis, noting that pressure changes would primarily be seen on the near offset seismic data, to partition pressure and saturation effects. Their analysis yields a similar conclusion to our findings.

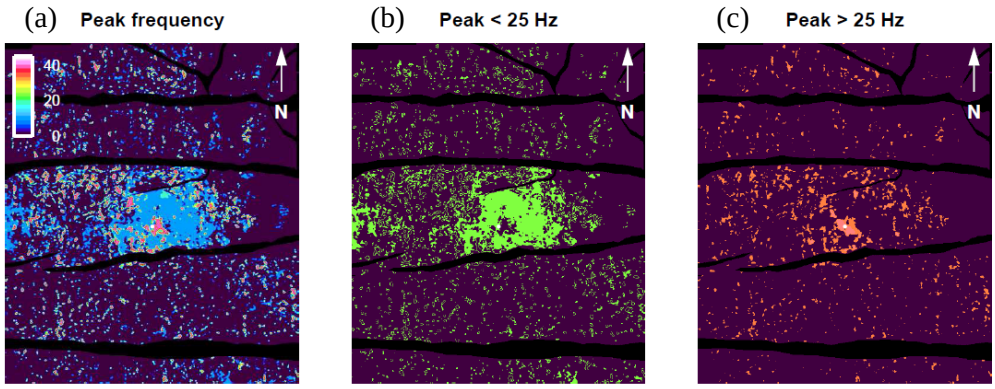

Figure 4. *(a)Frequency displaying the greatest change in reflection amplitude between pre- and post-injection 3D seismic surveys. (b) and (c) split the data either side of a 25 Hz cut-off to separate pressure and saturation changes.*

Conclusions

Spectral decomposition has been used to discriminate between direct fluid substitution and pressure changes in the storage reservoir. A clear change in the lateral extent of the peak tuning reflection amplitudes is seen between low and high frequency components of the wavefield. The results show agreement with previous attempts, using different methods, to differentiate between CO_2 saturation changes and pressure increases in the Tubaen caused by injection (Hansen et al., 2001).

Acknowledgements

This publication has been produced with support from the BIGCCS Centre, performed under the Norwegian research program Centres for Environment-friendly Energy Research (FME). This paper is published with the permission of the Executive Director, British Geological Survey (NERC).

References

Hansen, O., Eiken, O., Ostmo, S. and Inge Johansen, R. [2011] Monitoring CO_2 injection into a fluvial brine-filled sandstone formation at the Snohvit field, Barents Sea. SEG Annual Meeting, San Antonio.

Partyka, G., Grigley, J. and Lopez, J. [1999] Interpretational applications of spectral decomposition in reservoir characterization. The Leading Edge, 18, 353–360.

Williams, G.A. and Chadwick, R.A. [2012] Quantitative seismic analysis of a thin layer of CO_2 in the Sleipner injection plume. Geophysics, 77 (6), R245-R256.

White, J.C., Williams, G.A. and Chadwick, R.A. [2013] Thin layer detectability in a growing CO_2 plume: testing the limits of time-lapse seismic resolution. Energy Procedia, 37, 4356-4365.